DMD Fast Forward. Published on July 8, 2005 as doi:10.1124/dmd.105.005413

A SIMPLE SEQUENTIAL INCUBATION METHOD FOR DECONVOLUTING THE COMPLICATED SEQUENTIAL METABOLISM OF CAPRAVIRINE IN HUMANS

Hai-Zhi Bu, Ping Kang, Ping Zhao, William F. Pool, and Ellen Y. Wu

Department of Pharmacokinetics, Dynamics & Metabolism (H.-Z.B., P.K., P.Z., W.F.P., E.Y.W.), Pfizer Global Research and Development, San Diego, California

a) Running Title:

MECHANISTIC STUDY OF CAPRAVIRINE METABOLISM

b) Contact Information of the Corresponding Author:

Hai-Zhi Bu, Ph.D.

Department of Pharmacokinetics, Dynamics and Metabolism, Pfizer Global Research and Development, San Diego, CA 92121.

Tel: 1-858-622-7985

Fax: 1-858-622-5999

Email: haizhi.bu@pfizer.com

c) Numerical Information of the Manuscript:

The number of Text Pages:	13
The number of Tables:	0
The number of Figures:	8
The number of References:	7
The number of Words in the *Abstract*:	250
The number of Words in the *Introduction*:	239
The number of Words in the *Discussion*:	441

d) Abbreviations Used in the Manuscript:

HIV, human immunodeficiency virus; NADPH, β-nicotinamide adenine dinucleotide phosphate reduced tetrasodium salt; CYP, cytochrome P450; HPLC, high-performance liquid chromatography; LC-MS, liquid chromatography-ion-trap mass spectrometry; RAM, radioactivity monitoring; ESI, electrospray ionization.

ABSTRACT:

Capravirine, a non-nucleoside reverse transcriptase inhibitor for the treatment of HIV type 1, undergoes extensive oxygenations to numerous sequential metabolites in humans. Since several possible oxygenation pathways may be involved in the formation and/or sequential metabolism of a single metabolite, it is very difficult or even impossible to determine the definitive pathways and their relative contributions to the overall metabolism of capravirine using conventional approaches. For this reason, a human liver microsome-based *sequential incubation* method has been developed to deconvolute the complicated sequential metabolism of capravirine. Briefly, the method includes three fundamental steps: 1) 30-min primary incubation of [^{14}C]capravirine, 2) isolation of [^{14}C]metabolites from the primary incubate, and 3) 30-min sequential incubation of each isolated [^{14}C]metabolite supplemented with an ongoing (30 min) microsomal incubation with non-labeled capravirine. Based on the extent of both the disappearance of the isolated precursor [^{14}C]metabolites and the formation of sequential [^{14}C]metabolites, definitive oxygenation pathways of capravirine were assigned. In addition, the percent contribution of a precursor metabolite to the formation of each of its sequential metabolites (called sequential contribution) and the percent contribution of a sequential metabolite formed from each of its precursor metabolites (called precursor contribution) were determined. An advantage of this system is that the sequential metabolism of each isolated [^{14}C]metabolite can be monitored selectively by radioactivity in the presence of all relevant metabolic components (i.e., non-labeled parent and its other metabolites). This methodology should be applicable to mechanistic

studies of other compounds involving complicated sequential metabolic reactions when radiolabeled materials are available.

Capravirine (AG1549 or S-1153), 2-carbamoyloxymethyl-5-(3,5-dichlorophenyl)thiol-4-isopropyl-1-(4-pyridyl)methyl-1*H*-imidazole, is a new non-nucleoside reverse transcriptase inhibitor under development for the oral treatment of human immunodeficiency virus (HIV) type 1 (De Clercq, 2001, 2002; Fujiwara et al., 1998, 1999; Ohkawa et al., 1998; Ren et al., 2000). Capravirine undergoes extensive oxygenation reactions in humans following oral administration of capravirine alone or in combination with ritonavir (Bu et al., 2004). The oxygenation pathways of capravirine in humans are restricted to *N*-oxidation at the pyridinyl nitrogen atom, sulfoxidation, and primary/tertiary hydroxylation at the isopropyl group. Four primary (mono-oxygenated) and numerous sequential (di-, tri-, and tetra-oxygenated) metabolites of capravirine are formed via the aforementioned individual or combined oxygenation pathways (Fig. 1). Since these sequential oxygenation pathways are highly cross-linked (i.e., multiple pathways are involved in the formation and/or sequential metabolism of a single metabolite), it is very difficult or even impossible to determine the relative contribution of each pathway using conventional approaches. The purpose of this study was to determine definitive oxygenation pathways of capravirine and assess the percent contribution of a precursor metabolite to the formation of each of its sequential metabolites (called sequential contribution) as well as the percent contribution of a sequential metabolite formed from each of its precursor metabolites (called precursor contribution). The [^{14}C]capravirine/human liver microsome-based *sequential incubation* methodology that we developed can be a general approach to characterizing sequential biotransformation reactions of other chemical/biochemical compounds and drugs when radiolabeled materials are available.

Materials and Methods

Materials. [^{14}C]capravirine (>99% radiochemical purity) was synthesized at Pfizer (St. Louis, MO). Human liver microsomes (pooled from 14 donors) were prepared at Pfizer (Groton, CT). All other commercially available reagents and solvents were of either analytical or high performance liquid chromatography (HPLC) grade.

Microsomal Metabolism. [^{14}C]Capravirine (2 μM) was incubated for 0 to 60 min at 37 °C in an incubation system comprised of 100 mM potassium phosphate buffer (pH 7.4), human liver microsomes (0.2 mg/ml), and 1 mM β-nicotinamide adenine dinucleotide phosphate reduced tetrasodium salt (NADPH) in a final volume of 1 ml. After 5-min preincubation, reactions were initiated by the addition of NADPH and terminated by the addition of 2 ml ice-cold acetonitrile. Samples were vortexed and then centrifuged for 5 min. The supernatant from each incubation tube was transferred into an appropriate polypropylene tube for evaporation to dryness under N_2 at 40 °C. The dried residues were reconstituted in 110 μl of 30:70 (v/v) methanol:20 mM ammonium acetate (pH 4) and an aliquot (100 μl) of each reconstituted solution was injected into an HPLC-MS-RAM system, as described in the following Metabolite Profiling section, for analysis.

Sequential Incubation. Initially, [^{14}C]capravirine (2 μM) was incubated with human liver microsomes (0.2 mg/ml) for 30 min at 37 °C (called primary incubation; two 1-ml replicates). All other incubation conditions and sample preparation procedures were the same as described in the Microsomal Metabolism section. The reconstituted solution (total 1 ml) pooled from the two primary incubation tubes was injected at a volume of 0.9 ml for the isolation of [^{14}C]metabolites using the HPLC method as described in the following Metabolite Profiling

DMD Fast Forward. Published on July 8, 2005 as DOI: 10.1124/dmd.105.005413
This article has not been copyedited and formatted. The final version may differ from this version.

section. Each [^{14}C]metabolite of interest was collected using a Gilson FC 204 fraction collector (Middleton, WI). The fraction collected for each [^{14}C]metabolite (with the exception that [^{14}C]C4, [^{14}C]C18, and [^{14}C]C22 were pooled to generate a [^{14}C]metabolite mixture) was split equally into two incubation tubes that were evaporated to dryness under N_2 at 40 °C.

Non-labeled capravirine (2 μM) was incubated with human liver microsomes for 30 min (called supplemental incubation; as many 1-ml replicates as needed). All other incubation conditions were identical to those for the primary incubation. At 30 min, a 1-ml ongoing supplemental incubation (not terminated) was quickly transferred into each of the two aforementioned dried tubes containing the isolated [^{14}C]metabolite(s). After vortexing (5 s), one tube was terminated immediately by the addition of 2 ml ice-cold acetonitrile (control). The other tube was incubated for an additional 30 min at 37 °C (called *sequential incubation*) and then terminated by the addition of 2 ml ice-cold acetonitrile. The same sequential incubation procedure was executed for each isolated [^{14}C]metabolite of interest. All subsequent sample preparation procedures were the same as described in the Microsomal Metabolism section, except that dried residues were reconstituted in 1 ml of 30:70 (v/v) methanol:20 mM ammonium acetate (pH 4). An aliquot (0.9 ml) of each reconstituted solution was injected into the HPLC-MS-RAM system for analysis.

Metabolite Profiling. Metabolite profiling was performed on an Agilent 1100 HPLC system (Wilmington, DE) coupled with an IN/US Model 3 β-RAM radio-detector (Tampa, FL), an ARC Model C StopFlow system (AIM Research Company, Newark, DE), and a Finnigan LCQ-Deca ion-trap mass spectrometer (San Jose, CA). An Agilent 1100 autosampler used in the study was upgraded with a 900-μl injection loop and pump head. Thus, a maximal volume of 900 μl could be singly injected. Separation was achieved using a Phenomenex Aqua C18 column

(150 × 4.6 mm, 5μ) at a flow rate of 1.0 ml/min. The effluent was split to allow 20% to the mass spectrometer via the supplied electrospray ionization (ESI) source and 80% to mix with either Packard BioScience ULTIMA FLO-M scintillation cocktail (Meriden, CT) at 2.4 ml/min or ARC StopFlow AD scintillation cocktail (AIM Research Company, Newark, DE) at 1.2 ml/min and then flow through the radio-detector. A mobile phase gradient of (A) 20 mM ammonium acetate (pH 4) and (B) methanol was programmed as follows: initiated with 100% A for 10 min, changed to 60% A from 10 to 30 min, changed to 55% A from 30 to 35 min, held at 55% A from 35 to 60 min, changed to 40% A from 60 to 70 min, changed to 10% A from 70 to 80 min, held at 10% A from 80 to 90 min, changed to 100% A from 90 to 92 min, and held at 100% A from 92 to 100 min for column equilibration. All above gradient changes were linear. Major operating parameters for the ion-trap ESI-MS method were as follows: positive ion mode with a spray voltage of 4.5 kV, capillary temperature of 200°C, sheath gas flow rate of 70 (arbitrary), and an auxiliary gas flow rate of 20 (arbitrary). Laura 3 V3.0 (IN/US Systems, Tampa, FL), ARC data system Version 2.4 (AIM Research Company, Newark, DE) and Xcalibur V1.4 (ThermoFinnigan, San Jose, CA) were used to control the β-RAM detector, the StopFlow system and the LC-MS system, respectively, for data acquisition and processing. The metabolite profiling of sequential incubations of the isolated [^{14}C]metabolites was performed using the StopFlow system-controlled radio-detector, where time intervals were preset for stop-flow radiochemical detection in terms of known metabolite information. Outside the preset intervals, no radiochemical detection was executed. The ARC StopFlow-controlled radio-detector is 10-20 fold more sensitive than the conventional flow-through detection method (Nassar et al., 2003). However, it takes a much longer time to finish a run because the system stops the flow for radioactivity counting during most of the run time (stop for 60 s per every 8 s in this study).

DMD Fast Forward. Published on July 8, 2005 as DOI: 10.1124/dmd.105.005413
This article has not been copyedited and formatted. The final version may differ from this version.

Data Analysis. Based on the extent of both the disappearance of isolated precursor [^{14}C]metabolites and the formation of corresponding sequential [^{14}C]metabolites, definitive oxygenation pathways were readily assigned. Two new terms, *sequential contribution* and *precursor contribution*, are described as follows:

1. *Sequential contribution* represents the percent contribution of a precursor metabolite to the formation of each of its sequential metabolites when the precursor metabolite is metabolized to two or more sequential metabolites. For example, a precursor metabolite, PM, is metabolized to two sequential metabolites, SM1 and SM2. The percent contribution of PM to the formation of SM1 or SM2 during the sequential incubation course can be calculated:

$$\%\text{Contribution (PM-to-SM1)} = [A_{SM1}/(A_{SM1} + A_{SM2})] \times 100\%$$

$$\%\text{Contribution (PM-to-SM2)} = [A_{SM2}/(A_{SM1} + A_{SM2})] \times 100\%$$

where $A_{SM1}$and A_{SM2} represent the radiochromatographic peak area (or radioactivity) of SM1 and SM2, respectively.

2. *Precursor contribution* represents the percent contribution of a sequential metabolite formed from each of its precursor metabolites when the sequential metabolite is formed from two or more precursor metabolites. For example, a sequential metabolite, SM, is formed from two precursor metabolites, PM1 and PM2. The percent contribution of SM formed from PM1 or PM2 during the sequential incubation course can be calculated:

$$\%\text{Contribution (SM-from-PM1)} = [A_{SM\text{-from-}PM1}/(A_{SM\text{-from-}PM1} + A_{SM\text{-from-}PM2})] \times 100\%$$

$$\%\text{Contribution (SM-from-PM2)} = [A_{SM\text{-from-}PM2}/(A_{SM\text{-from-}PM1} + A_{SM\text{-from-}PM2})] \times 100\%$$

where $A_{SM\text{-}from\text{-}PM1}$ and $A_{SM\text{-}from\text{-}PM2}$ represent the radiochromatographic peak area (or radioactivity) of SM formed from PM1 and PM2, respectively.

DMD Fast Forward. Published on July 8, 2005 as DOI: 10.1124/dmd.105.005413
This article has not been copyedited and formatted. The final version may differ from this version.

Results

Microsomal Metabolism of Capravirine. Capravirine was extensively oxygenated to a variety of primary and sequential metabolites in human liver microsomes (Fig. 2). Note that all metabolites observed in this *in vitro* study were identified in our previous study (Bu et al., 2004). In the current study, the identity of the *in vitro* metabolites was confirmed simply by the similarity in retention times and MS^2 ion-trap mass spectra between the *in vitro* and *in vivo* data. The primary metabolites (mono-oxygenated) were formed via sulfoxidation (metabolite C23), *N*-oxidation at the pyridinyl nitrogen atom (metabolite C26), and tertiary hydroxylation (metabolite C19) and primary hydroxylation (metabolite C20) at the isopropyl group. All sequential metabolites (di-, tri-, and tetra-oxygenated) were formed via combinations of the four types of mono-oxygenation reactions (Fig. 1).

Following the incubation of [^{14}C]capravirine in human liver microsomes, the oxygenation-time courses of the parent and its metabolites are shown in Fig. 3. It should be noted that metabolites C19, C20 and C25b were present at trace/minor levels over the entire incubation time. In contrast, C23 and C26 represent the two most abundant metabolites of capravirine in human liver microsomes. All other metabolites have low to moderate abundances (Fig. 3).

Sequential Incubation. The primary incubations of [^{14}C]capravirine in human liver microsomes were conducted in order to generate [^{14}C]metabolites. The [^{14}C]metabolites with sufficient abundances were isolated for sequential incubations. Note that ~70% of each [^{14}C]metabolite in the primary incubation was isolated for its sequential incubation. The isolated [^{14}C]metabolites from the primary incubations included C4, C9, C15, C18, C22, C23, and C26. The [^{14}C]metabolites C3 and C11 were not isolated because they did not show any sequential metabolism. The [^{14}C]metabolites C19, C20 and C25b were not isolated directly from the

primary incubations because of their low abundances (<1% of total radioactivity, Fig. 2). However, the [^{14}C]metabolite C25b, which might undergo sequential oxygenations, was isolated from a surrogate incubation of [^{14}C]capravirine in dog CYP3A12 supersomes in which C25b was formed at a sufficient amount for isolation (data not shown). The supplemental incubations of non-labeled capravirine in human liver microsomes were conducted in order to generate ongoing incubation mixtures for sequential incubations of the isolated [^{14}C]metabolites. When an isolated [^{14}C]metabolite was mixed with an ongoing supplemental incubation, the sequential incubation of the [^{14}C]metabolite was conducted under conditions that mimicked continued incubation of the supplemental mixture. Thus, the sequential incubation method has the ability to monitor selectively, by radioactivity, the disappearance of each isolated [^{14}C]metabolite and the appearance of its sequential [^{14}C]metabolite(s) in the presence of all relevant metabolic components (non-labeled). It should be noted that the incubation time of 30 min for each of the primary, supplemental and sequential incubations was selected based on the oxygenation-time courses of capravirine and its metabolites (Fig. 3). The total radioactivity measured from the 30-min sequential incubations (Figs. 4-8 B panels) was 97-108% of that measured from the 0-min sequential incubations (Figs. 4-8 A panels). In addition, it was assumed that the concentrations of the added [^{14}C]metabolites would not cause significant changes in metabolic rates under the linear conditions (Fig. 3).

Metabolite [^{14}C]C23 underwent extensive oxygenations to a variety of sequential metabolites with a metabolite profile similar to that of [^{14}C]capravirine for all applicable metabolites (Fig. 4 vs. Fig. 2), suggesting that C23 represents the most important mono-oxygenated metabolite responsible for the extensive sequential metabolism of capravirine in humans. In contrast, metabolite [^{14}C]C26 underwent minor metabolism to a major metabolite

DMD Fast Forward. Published on July 8, 2005 as DOI: 10.1124/dmd.105.005413
This article has not been copyedited and formatted. The final version may differ from this version.

C15 and a trace metabolite C4 (Fig. 5), suggesting a minor role of C26 in the overall sequential oxygenations of capravirine.

Metabolite [^{14}C]C9 underwent extensive sequential biotransformation with a metabolite profile similar to that of [^{14}C]capravirine for all applicable metabolites (Fig. 6 vs. Fig. 2). This suggested that C9 represents an important di-oxygenated metabolite responsible for sequential tri- and tetra-oxygenations of capravirine in humans. In contrast, metabolite [^{14}C]C15 only underwent trace-level sequential metabolism to C4 (Fig. 7), suggesting a negligible role of C15 in sequential oxygenations of capravirine in humans. In addition, the sequential incubation of metabolite [^{14}C]C25b indicated that C25b was sequentially oxygenated to C22 only (data not shown).

Theoretically, each of the three tri-oxygenated metabolites [^{14}C]C4, [^{14}C]C18 and [^{14}C]C22 may be further oxygenated to the tetra-oxygenated metabolite C11 only. Therefore, the relative contributions of the three metabolites to the formation of C11 can be estimated based on the extent of the disappearance of [^{14}C]C4, [^{14}C]C18 and [^{14}C]C22. All three [^{14}C]metabolites were co-incubated to evaluate their sequential metabolism (Fig. 8). After the 30-min sequential co-incubation, both [^{14}C]C4 and [^{14}C]C22 did not show any disappearance while [^{14}C]C18 completely disappeared (Fig. 8), suggesting that only C18 undergoes further oxygenation to C4.

Based on the above sequential incubation results of the isolated [^{14}C]metabolites, the definitive oxygenation pathways were assigned and the relative contributions of the pathways during the sequential incubation course were estimated for the extensive metabolism of capravirine in human liver microsomes (Fig. 1). Generally, it was straightforward to perform the pathway assignments and the estimations of relative contributions using the methods described in the Data Analysis section. One exception was the difficulty in estimating the sequential

contributions of C23 to its direct sequential metabolites C9, C15 and C25b, due to their further sequential oxygenations. Following the sequential incubation of [^{14}C]C23 in human liver microsomes, the sum of the abundances of C22 and C25b represented the sequential contribution of C23 to C25b, the sum of the abundance of C15 and 10% of C4 was the sequential contribution of C23 to C15, and the sum of the abundances of C9, C3, C18 and C11 and 90% of C4 accounted for the sequential contribution of C23 to C9. Thus, the sequential contributions of C23 to C25b, C15 and C9 during the sequential incubation course were calculated to be 17%, 31% and 52%, respectively, by the normalization of the three individual sums (Fig. 1). Likewise, the percent contributions of capravirine to the formations of the four mono-oxygenated metabolites C19, C20, C23 and C26 were estimated based on the time courses of the parent disappearance and metabolite formation in the incubations of [^{14}C]capravirine in human liver microsomes (Figs. 1 and 3).

Discussion

For a drug undergoing extensive sequential metabolism via numerous metabolic pathways, it is very difficult or even impossible to identify definitive pathways and determine the relative contribution of each pathway to the total metabolism of the drug using conventional approaches such as performing individual incubations of synthetic or isolated metabolites (radiolabeled or non-labeled) in liver microsomes and hepatocytes. Based on *in vitro* studies using synthetic non-labeled metabolites, possible tentative pathways can be proposed but relative contributions of these pathways cannot be determined. In practice, it is very expensive, time-consuming or even infeasible to synthesize all metabolites of a compound. Alternatively, radiolabeled metabolites of a compound can be isolated from *in vitro* incubations and/or *in vivo* samples after dosing of the radiolabeled compound. By conducting individual incubations of the isolated radiolabeled metabolites, possible metabolic pathways can be proposed and sequential contributions of these pathways can be determined. Since the above sequential metabolism studies of the individual metabolites are usually conducted both at concentrations irrelevant to their abundances in primary incubations and in the absence of other metabolic components (the parent and its other metabolites), the data obtained through the conventional *in vitro* approaches can only be tentative or may be irrelevant to the observations from the primary incubations.

Ideally, a sequential incubation of a precursor metabolite should be performed in an incubation medium containing the same metabolic components as in the incubation medium of the parent drug where all relevant parent-metabolite/metabolite-metabolite interactions are maintained. Allowing sequential metabolism to occur in the natural incubation milieu ensures the relevance of the data obtained. The *sequential incubation* methodology developed in the present study is composed of three steps: 1) 30-min primary incubation of [^{14}C]capravirine, 2) isolation

of [^{14}C]metabolites of interest from the incubate, and 3) 30-min sequential incubation of each isolated [^{14}C]metabolite supplemented with an ongoing (30 min) microsomal incubation with non-labeled capravirine. The strategically-designed 3-step process ensures that all sequential liver microsomal incubations of the isolated [^{14}C]metabolites are conducted under the conditions that mimic the intact incubation of the parent drug.

This strategy for the mechanistic study of the sequential metabolism of capravirine in humans shows a number of advantages over the conventional approaches. These are summarized as follows: 1) no need for the synthesis of metabolite standards, 2) efficient isolation of all radiolabeled metabolites of interest from only two 1-ml microsomal incubations consuming minimal cost and time, 3) achieving definitive information on all metabolic pathways and the relative contribution of each pathway to the total metabolism of the parent, and 4) a readily usable method for the characterization of sequential biotransformation reactions of other chemical/biochemical compounds and drugs when radiolabeled materials are available.

Acknowledgments. We would like to acknowledge Drs. Deepak Dalvie, James Ferrero, Wei-Zhu Zhong and Geoffrey Peng for their reviews of this manuscript.

References

Bu H-Z, Pool WF, Wu EY, Raber SR, Amantea MA and Shetty BV (2004) Metabolism and excretion of capravirine, a new non-nucleoside reverse transcriptase inhibitor, alone and in combination with ritonavir in healthy volunteers. *Drug Metab Dispos* **32:**689–698.

De Clercq E (2001) New developments in anti-HIV chemotherapy. *Curr Med Chem* **8:**1543–1572.

De Clercq E (2002) Highlights in the development of new antiviral agents. *Mini Rev Med Chem* **2:**163–175.

Fujiwara T, Sato A, el-Farrash M, Miki S, Abe K, Isaka Y, Kodama M, Wu Y, Chen LB, Harada H, Sugimoto H, Hatanaka M and Hinuma Y (1998) S-1153 inhibits replication of known drug-resistant strains of human immunodeficiency virus type 1. *Antimicrob Agents Chemother* **42:**1340–1345.

Fujiwara T, Sato A, Patick AK and Potts KE (1999) In vitro antiviral activity and resistance profile of AG1549 (S-1153), a new non-nucleoside inhibitor of HIV-1 reverse transcriptase. *Int Antiviral News* **7:**18–20.

Nassar AEF, Bjorge SM and Lee DY (2003) On-line liquid chromatography-accurate radioisotope counting coupled with a radioactivity detector and mass spectrometer for metabolite identification in drug discovery and development. *Anal Chem* **75:**785–790.

Ohkawa T, Goto S, Miki S, Sato A, Kuroda T, Iwatani K, Takeuchi M and Nakano M (1998) Structural determination of metabolites of S-1153, a new, potent, non-nucleoside, anti-HIV agent in rat liver microsomes. *Xenobiotica* **28:**877–886.

Ren J, Nichols C, Bird LE, Fujiwara T, Sugimoto H, Stuart DI and Stammers DK (2000) Binding of the second generation non-nucleoside inhibitor S-1153 to HIV-1 reverse transcriptase involves extensive main chain hydrogen bonding. *J Biol Chem* **275:**14316–14320.

Legends for Figures

FIG. 1. Definitive metabolic scheme for oxygenations of capravirine in human liver microsomes.

Arrows indicate definitive pathways and an arrow with a cross mark represents a possible pathway proposed but not observed. The percentage at the end of an arrow indicates the sequential contribution while the percentage at the head of an arrow indicates the precursor contribution. No data shown at the end or head of an arrow indicates that the sequential or precursor contribution is 100% (or a single pathway responsible for the sequential metabolism or formation of a metabolite).

FIG. 2. A representative radiochromatogram generated from a 30-min primary incubation of [^{14}C]capravirine (2 μM) in human liver microsomes (0.2 mg/ml).

The radioactivity was detected using the regular (non-stop) radio-detector.

FIG. 3. Time courses of parent disappearance and metabolite formation in primary incubations of [^{14}C]capravirine (2 μM) in human liver microsomes (0.2 mg/ml).

The radioactivity was detected using the regular (non-stop) radio-detector.

FIG. 4. Representative metabolite profiles following sequential incubation of the isolated metabolite [^{14}C]C23 in human liver microsomes (0.2 mg/ml) for 0 min (A) and 30 min (B).

The radioactivity was detected using the StopFlow system controlled radio-detector with the preset stop-flow detection intervals. The flow was stopped for radiochemical detection for 60 s per every 8 s. Outside the preset intervals, no radiochemical detection was performed.

FIG. 5. Representative metabolite profiles following sequential incubation of the isolated metabolite [^{14}C]C26 in human liver microsomes (0.2 mg/ml) for 0 min (A) and 30 min (B).

The StopFlow radiochemical detection was the same as that described in Fig. 4.

FIG. 6. Representative metabolite profiles following sequential incubation of the isolated metabolite [^{14}C]C9 in human liver microsomes (0.2 mg/ml) for 0 min (A) and 30 min (B).

The StopFlow radiochemical detection was the same as that described in Fig. 4.

FIG. 7. Representative metabolite profiles following sequential incubation of the isolated metabolite [^{14}C]C15 in human liver microsomes (0.2 mg/ml) for 0 min (A) and 30 min (B).

The StopFlow radiochemical detection was the same as that described in Fig. 4.

FIG. 8. Representative metabolite profiles following sequential co-incubation of the three isolated metabolites [^{14}C]C4, [^{14}C]C18 and [^{14}C]C22 in human liver microsomes (0.2 mg/ml) for 0 min (A) and 30 min (B).

The StopFlow radiochemical detection was the same as that described in Fig. 4.

DMD Fast Forward. Published on July 8, 2005 as DOI: 10.1124/dmd.105.005413
This article has not been copyedited and formatted. The final version may differ from this version.

Figure 1

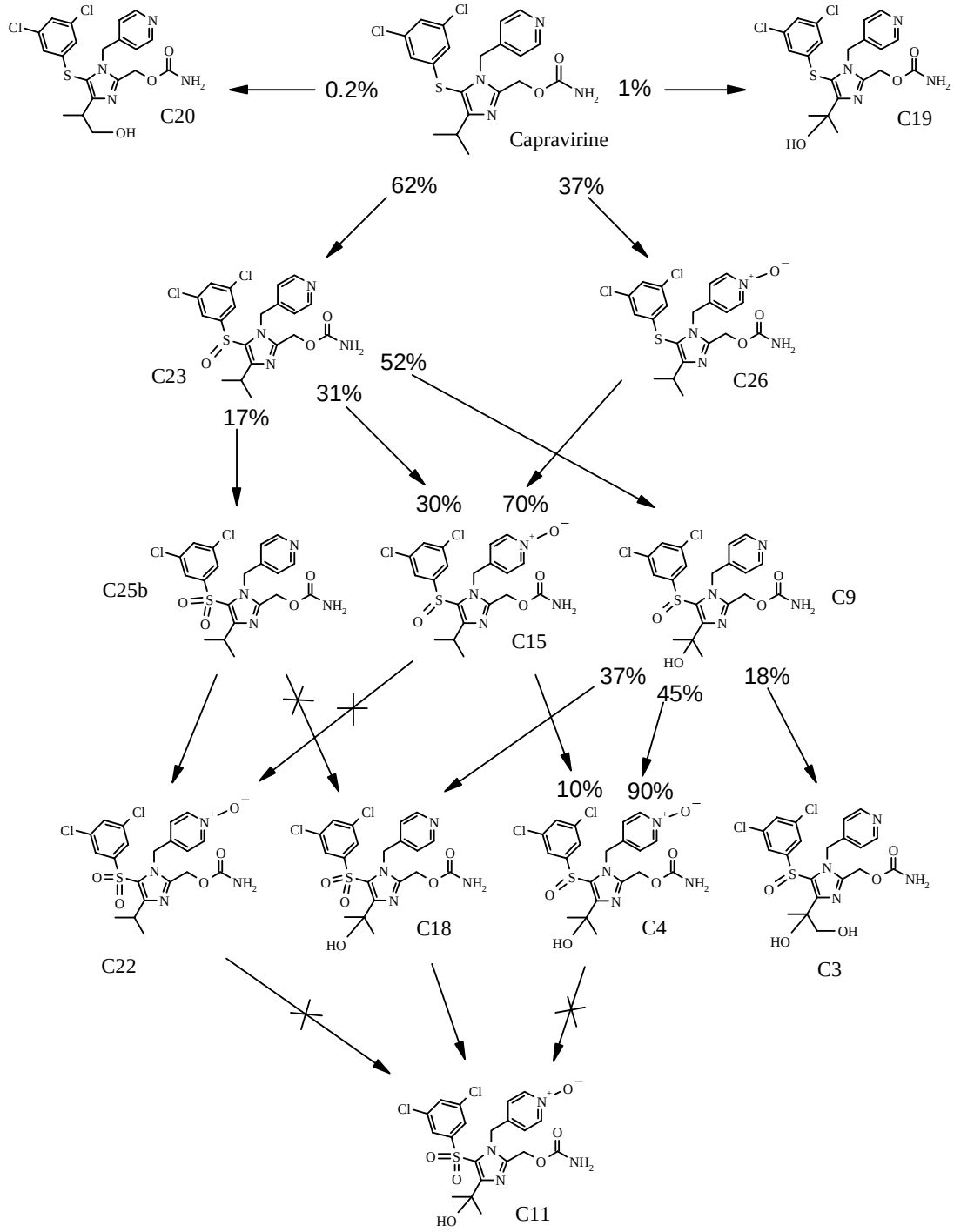

Figure 2

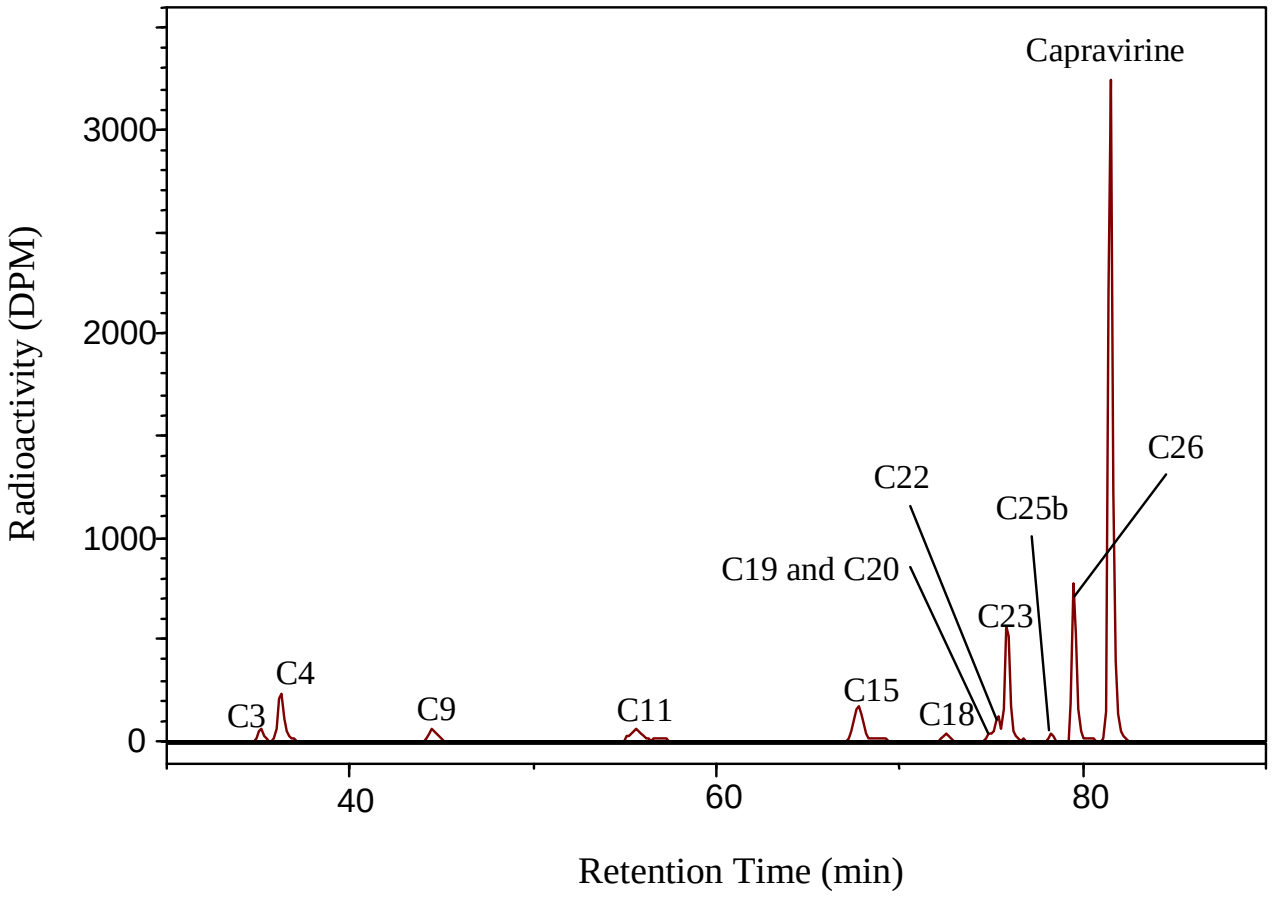

Figure 3

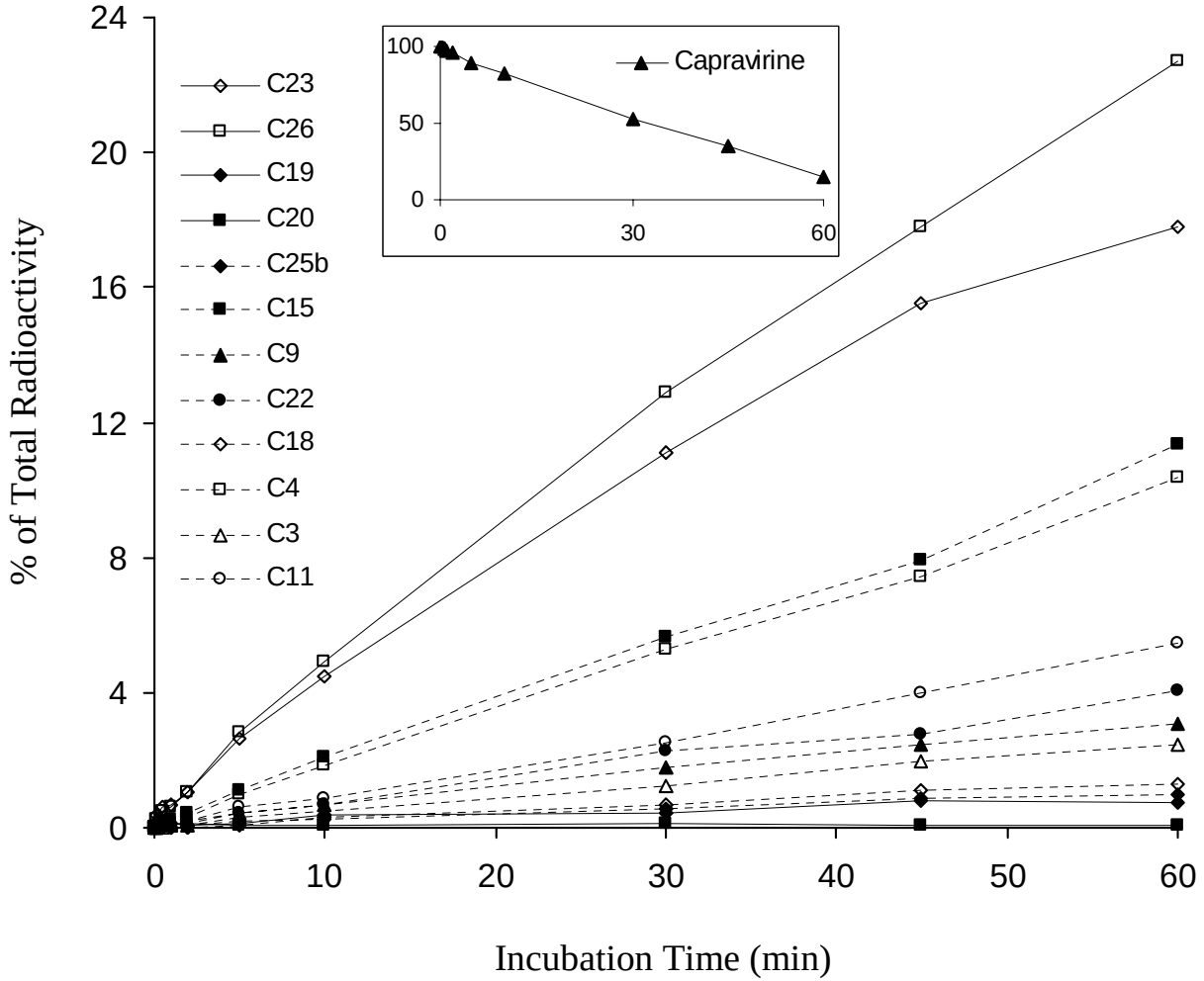

Figure 4

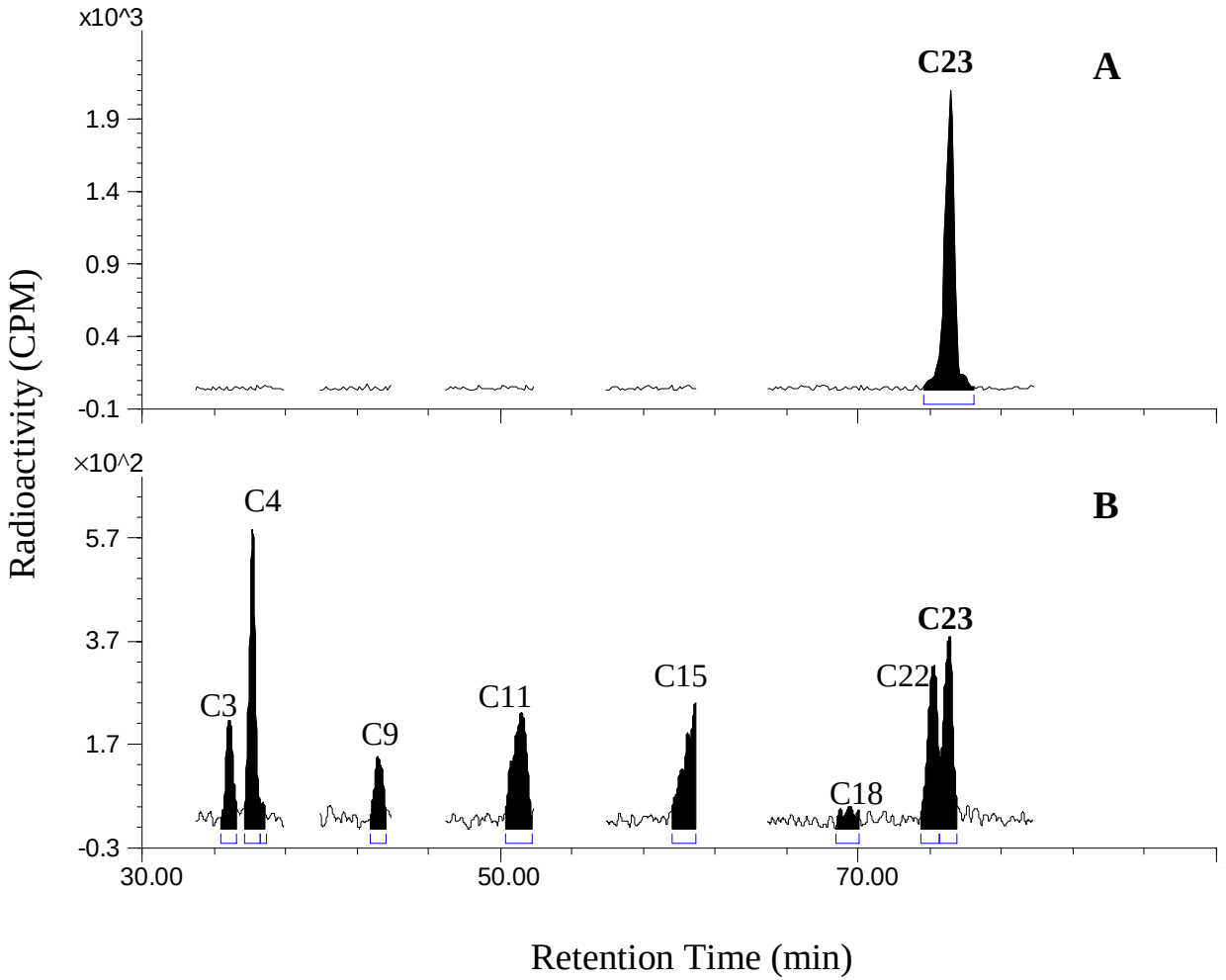

Figure 5

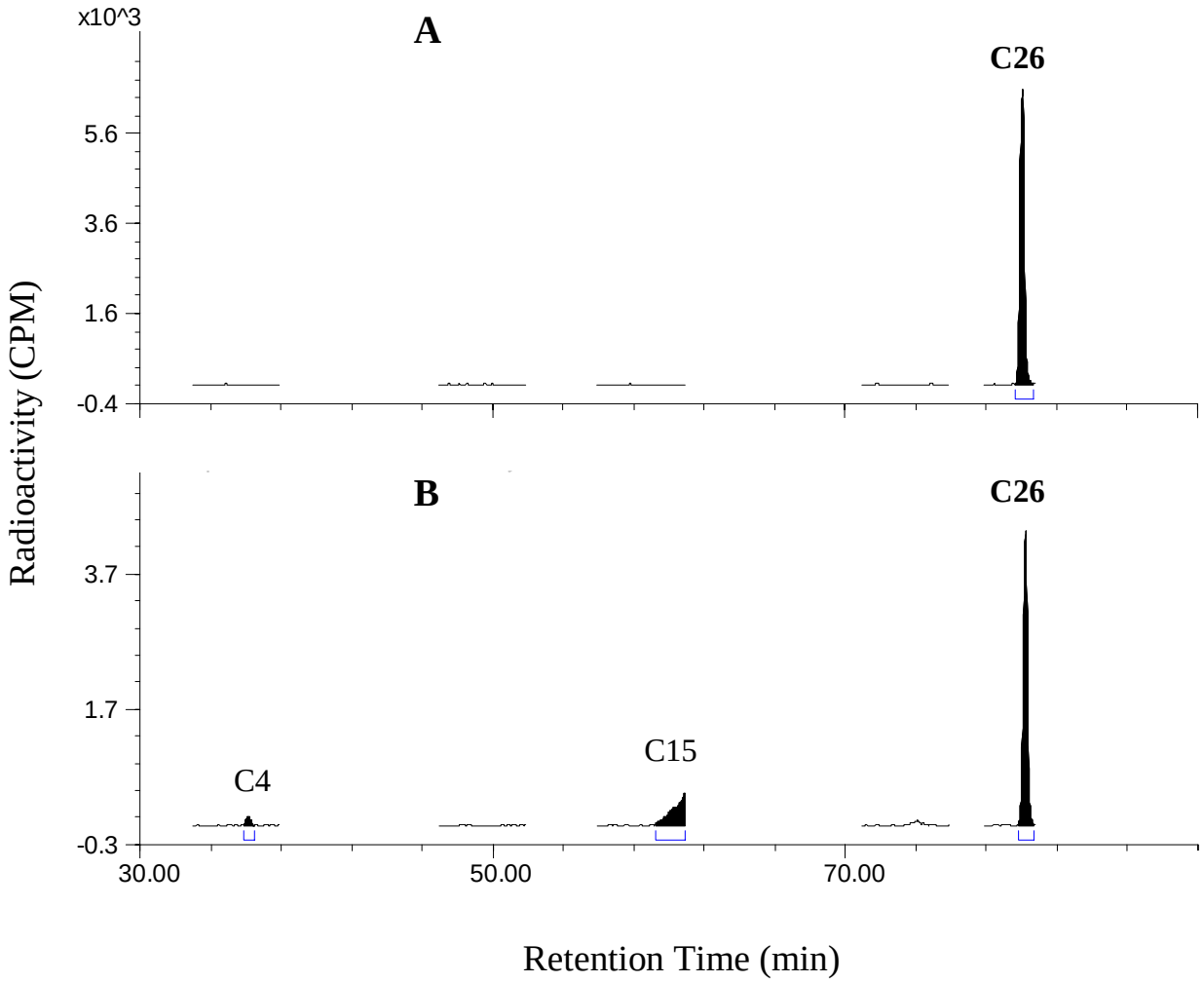

Figure 6

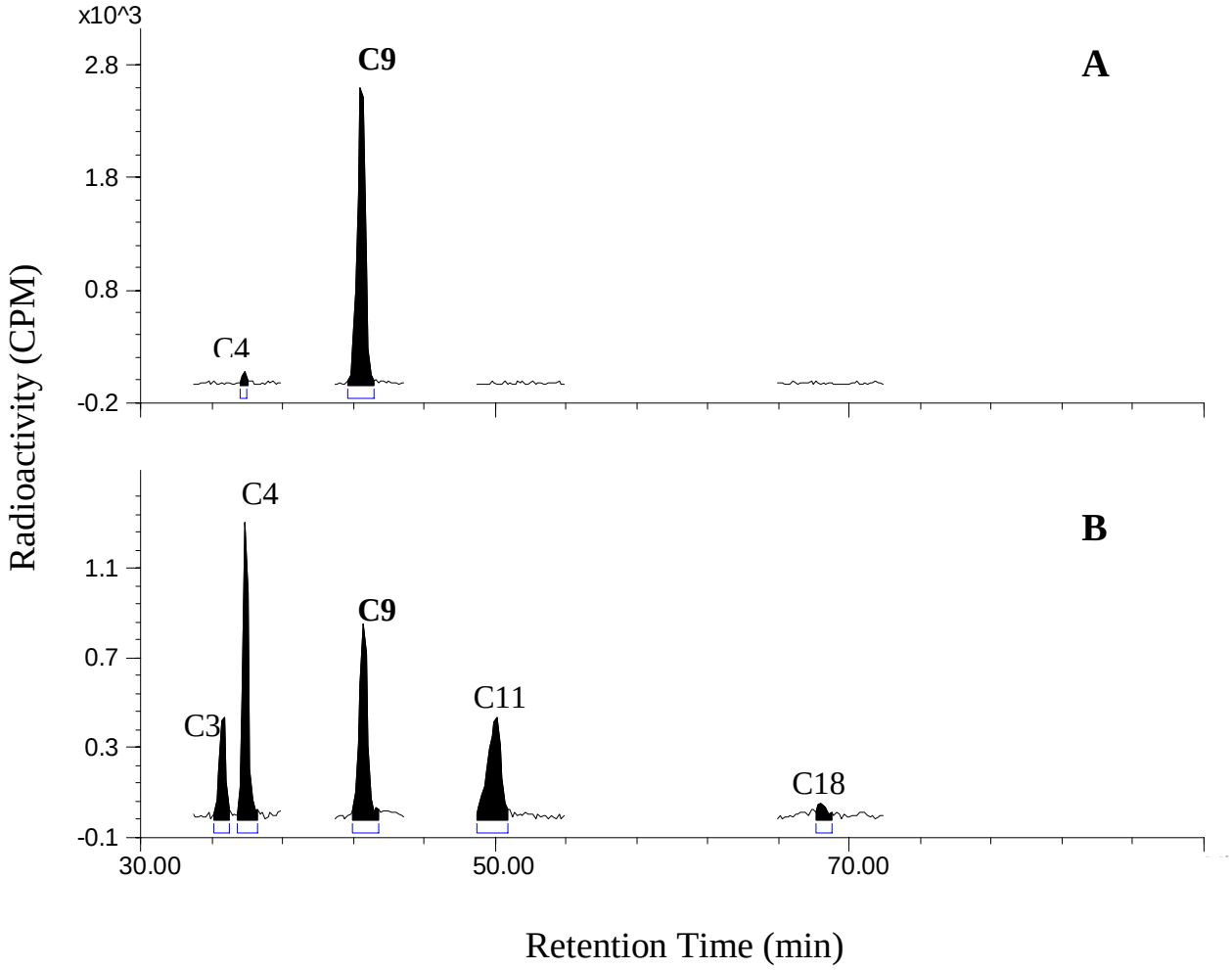

Figure 7

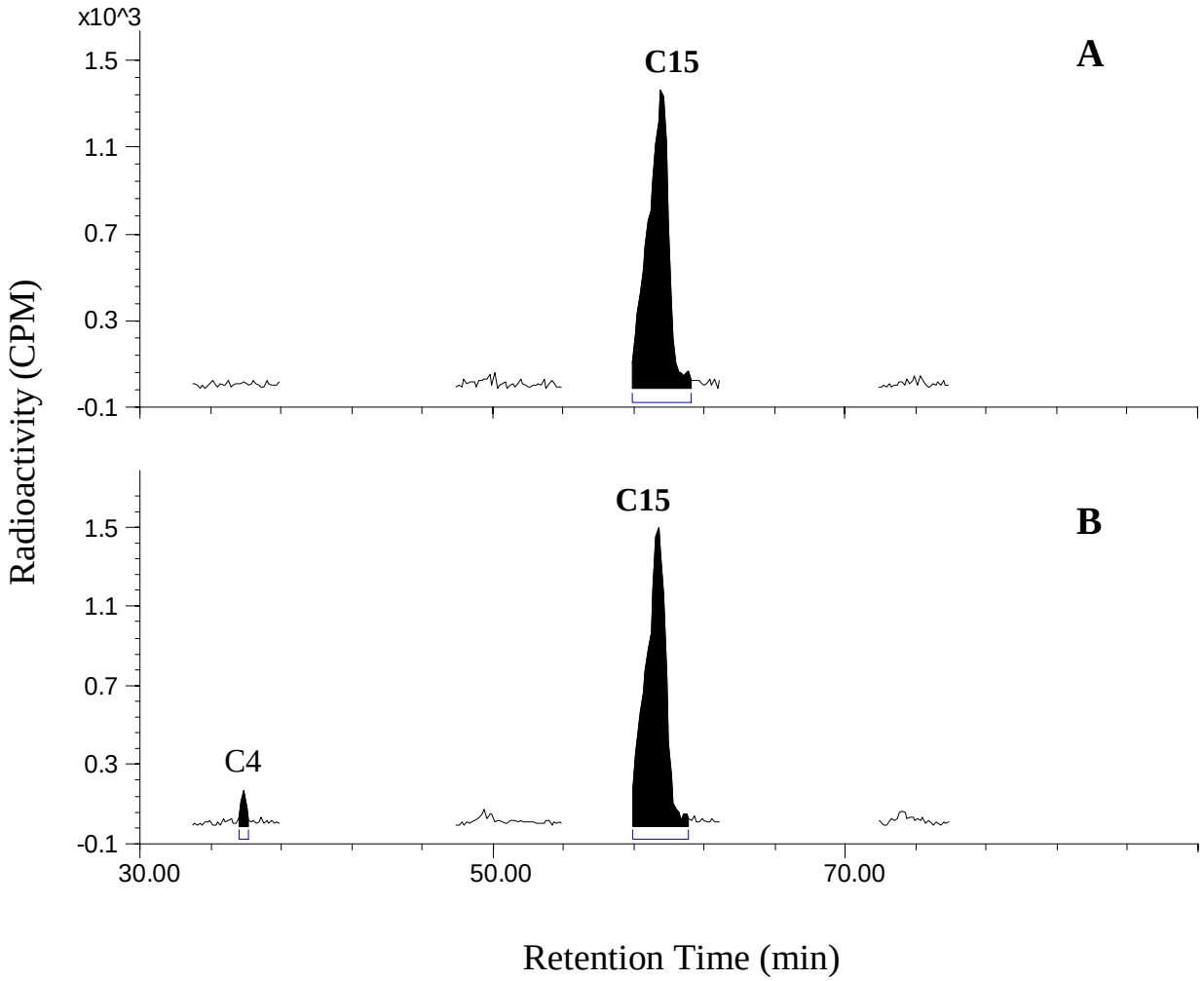

Figure 8